# Phosphoglycerate Kinases Are Co-Regulated to Adjust Metabolism and to Optimize Growth[1]

**Sara Rosa-Téllez,[a,b] Armand Djoro Anoman,[a,b] María Flores-Tornero,[a,b] Walid Toujani,[a,b] Saleh Alseek,[c] Alisdair R. Fernie,[c] Sergio G. Nebauer,[d] Jesús Muñoz-Bertomeu,[a,b] Juan Segura,[a,b] and Roc Ros[a,b,2]**

[a]Departament de Biologia Vegetal, Facultat de Farmàcia, Universitat de València, 46100 Valencia, Spain
[b]Estructura de Recerca Interdisciplinar en Biotecnologia i Biomedicina, Universitat de València, 46100 Burjassot, Spain
[c]Max Planck Institut für Molekulare Pflanzenphysiologie, 14476 Potsdam-Golm, Germany
[d]Departamento de Producción Vegetal, Universitat Politècnica de València, 46022 Valencia, Spain

**ORCID IDs: 0000-0002-6123-8173 (S.R.-T.); 0000-0003-0043-2180 (A.D.A.); 0000-0002-9296-0070 (M.F.-T.); 0000-0002-7971-9338 (W.T.); 0000-0003-2067-5235 (S.A.); 0000-0001-7978-6680 (S.G.N.); 0000-0002-2099-3754 (J.M.-B.); 0000-0001-7774-2676 (J.S.); 0000-0003-4254-8368 (R.R.).**

In plants, phosphoglycerate kinase (PGK) converts 1,3-bisphosphoglycerate into 3-phosphoglycerate in glycolysis but also participates in the reverse reaction in gluconeogenesis and the Calvin-Benson cycle. In the databases, we found three genes that encode putative PGKs. Arabidopsis (*Arabidopsis thaliana*) PGK1 was localized exclusively in the chloroplasts of photosynthetic tissues, while PGK2 was expressed in the chloroplast/plastid of photosynthetic and nonphotosynthetic cells. PGK3 was expressed ubiquitously in the cytosol of all studied cell types. Measurements of carbohydrate content and photosynthetic activities in PGK mutants and silenced lines corroborated that PGK1 was the photosynthetic isoform, while PGK2 and PGK3 were the plastidial and cytosolic glycolytic isoforms, respectively. The *pgk1.1* knockdown mutant displayed reduced growth, lower photosynthetic capacity, and starch content. The *pgk3.2* knockout mutant was characterized by reduced growth but higher starch levels than the wild type. The *pgk1.1 pgk3.2* double mutant was bigger than *pgk3.2* and displayed an intermediate phenotype between the two single mutants in all measured biochemical and physiological parameters. Expression studies in *PGK* mutants showed that *PGK1* and *PGK3* were down-regulated in *pgk3.2* and *pgk1.1*, respectively. These results indicate that the down-regulation of photosynthetic activity could be a plant strategy when glycolysis is impaired to achieve metabolic adjustment and optimize growth. The double mutants of *PGK3* and the triose-phosphate transporter (*pgk3.2 tpt3)* displayed a drastic growth phenotype, but they were viable. This implies that other enzymes or nonspecific chloroplast transporters could provide 3-phosphoglycerate to the cytosol. Our results highlight both the complexity and the plasticity of the plant primary metabolic network.

Glycolysis was the first metabolic pathway to be fully elucidated biochemically in the 1940s (Plaxton, 1996). It is a central pathway in most living organisms, where it provides energy in the form of ATP and reducing power, pyruvate to fuel the tricarboxylic acid cycle, and precursors for secondary metabolism, amino acid, and fatty acid biosynthesis (Plaxton, 1996). In plants, glycolysis is more complex than in animals, since it occurs independently in two compartments, the plastid and the cytosol. Besides, according to the genome databases (https://www.arabidopsis.org/), there is more than one isoform for each glycolytic reaction, and some of them are represented by more than 40 annotations. In spite of the important advances made in the functional characterization of both cytosolic and plastidial glycolytic enzymes (Sparla et al., 2005; Fermani et al., 2007; Muñoz-Bertomeu et al., 2009; Chen and Thelen, 2010; Prabhakar et al., 2010; Zhao and Assmann, 2011; Guo et al., 2012; Wakao et al., 2014), the relative contribution and the degree of integration of both pathways in different cell types are still far from being completely understood. In addition, some of the reactions of the plastidial glycolytic pathway are shared by the Calvin-Benson cycle, although operating in the opposite direction. Specifically, glyceraldehyde-3-phosphate dehydrogenase (GAPDH) and phosphoglycerate kinase (PGK) could participate in the same compartment and/or at the

[1] This work has been funded by the Spanish Government and the European Union: FEDER/ BFU2012-31519 and FEDER/ BFU2015-64204R, FPI fellowship to S.R.-T., and the Valencian Regional Government: PROMETEO II/2014/052.

[2] Address correspondence to roc.ros@uv.es.

The author responsible for distribution of materials integral to the findings presented in this article in accordance with the policy described in the Instructions for Authors (www.plantphysiol.org) is: Roc Ros (roc.ros@uv.es).

S.R.-T. performed most of the experiments and analyzed the data; A.D.A., M.F.-T., W.T., S.A., and S.G.N. performed some of the experiments and analyzed the data; A.R.F., J.S., and J.M.-B. supervised the experiments and provided technical assistance; R.R. conceived the project and wrote the article with contributions of J.S., A.R.F., S.G.N., and S.R.T.

www.plantphysiol.org/cgi/doi/10.1104/pp.17.01227

 

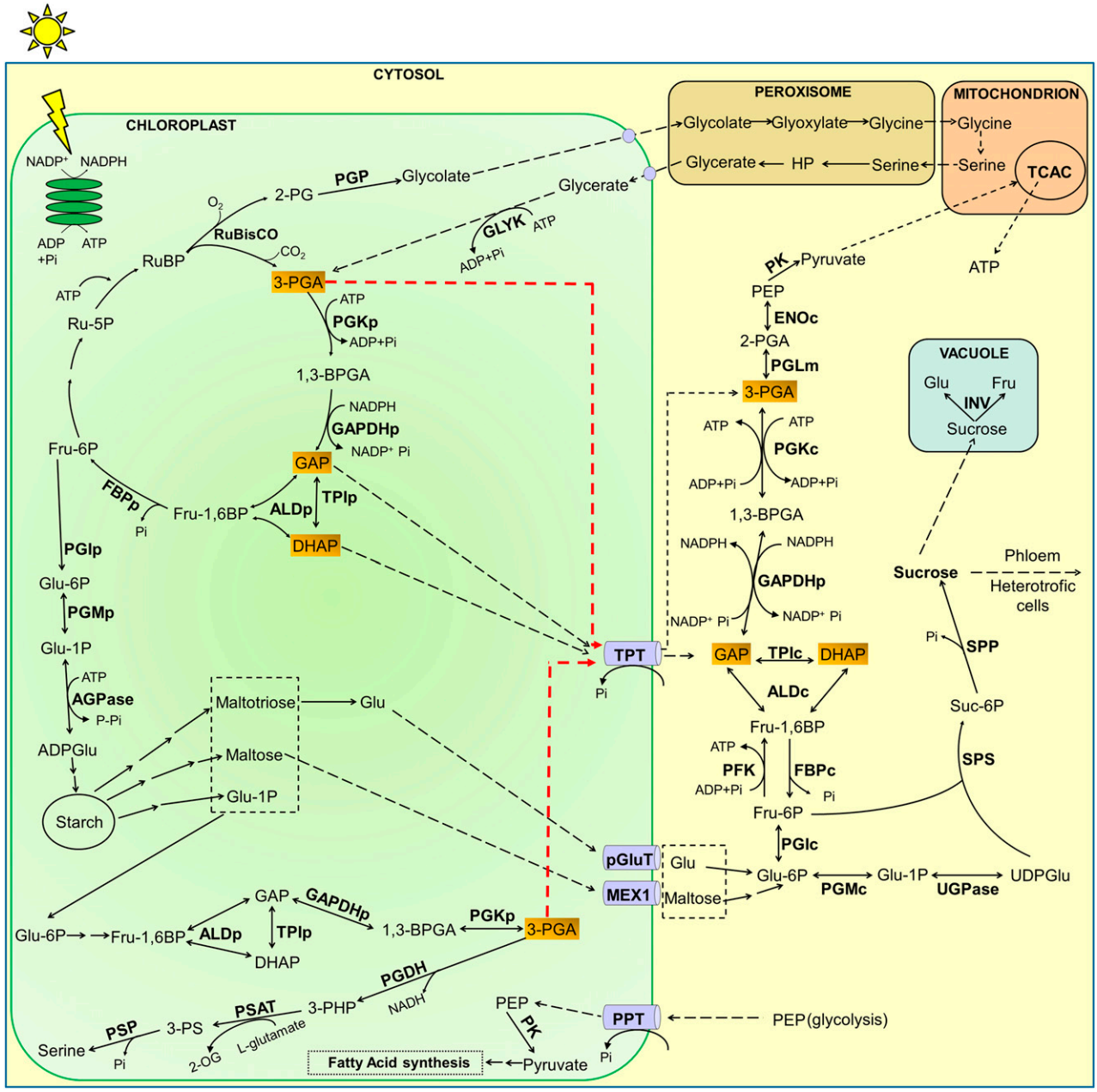


**Figure 1.** Schematic representation of the contribution of PGKs in the primary carbon metabolic pathways in photosynthetic cells. Abbreviations are as follows: 1,3-BPGA, 1,3-bis-phosphoglycerate; 2-OG, 2-oxoglutarate; 2-PG, 2-phosphoglycolate; 3-PGA, 3-phosphoglycerate; 3-PHP, 3-phosphohydroxypyruvate; 3-PS, 3-phosphoserine; ADPGlu, ADP-Glc; AGPase, ADP-Glc pyrophosphorylase; ALD, aldolase; DHAP, dihydroxyacetone phosphate; ENO, enolase; FBP, Fru-1,6-bisphosphatase; Fru-1,6BP, Fru-1,6- bisphosphate; GAP, glyceraldehyde 3-phosphate; GAPDH, glyceraldehyde 3-phosphate dehydrogenase; Glu-1P, Glc-1-P; Glu-6P, Glc-6-P; GLYK, glycerate kinase; HP, hydroxypyruvate; INV, vacuolar invertase; MEX1, maltose translocator; PEP, phospho*enol*pyruvate; PFK, phosphofructokinase; PGDH, 3-phosphoglycerate dehydrogenase; PGI, phosphoglucoisomerase; PGK, phosphoglycerate kinase; PGLm, phosphoglycerate mutase; pGluT, Glc translocator; PGM, Phosphoglucomutase; PGP, 2-phosphoglycolate phosphatase; PPT, phospho*enol*pyruvate translocator; PK, pyruvate kinase; PSAT, 3-phospho-Ser amino-transferase; PSP, 3-phospho-Ser phosphatase; Ru-5P, ribulose 5-phosphate; RuBP, ribulose 1,5-bisphosphate; SPP, Suc-6-P phosphatase; SPS, Suc phosphate synthase; TCAC, tricarboxylic acid cycle; TPI, triose phosphate isomerase; TPT, triose phosphate translocator; UDPGlu, UDP-Glc; UGPase, UDPGlu pyrophosphorylase; p or c after the enzyme name denotes the plastidial or cytosolic isoform, respectively. Discontinuous arrows represent fluxes between compartments. Hypothetical 3-PGA flux in *pgk3.2* is highlighted in red.

same time in photosynthetic and glycolytic/gluconeogenic reactions (Fig. 1). For this reason, the functional characterization of both GAPDH and PGK isoforms is of crucial importance.

Plant GAPDH isoforms have been characterized extensively at the genetic, biochemical, and molecular levels (Sparla et al., 2005; Hajirezaei et al., 2006; Fermani et al., 2007; Holtgrefe et al., 2008; Muñoz-Bertomeu et al., 2009, 2010; Guo et al., 2012, 2014; Anoman et al., 2015; Han et al., 2015). However, little attention has been paid to the functional characterization of PGKs. These enzymes are essential in the metabolism of most living organisms, and their sequence has remained highly conserved throughout evolution (Longstaff et al., 1989). They catalyze the reversible transfer of a highly energetic phosphate group at position 1 of the 1,3-bisphosphoglycerate to ADP to give rise to 3-phosphoglycerate (3-PGA) and ATP, and vice versa. PGKs from different species have been isolated in both animals and plants (Krietsch and Bücher, 1970; McCarrey and Thomas, 1987; Longstaff et al., 1989; Köpke-Secundo et al., 1990; McMorrow and Bradbeer, 1990; Löbler, 1998). Two PGK isoforms (PGK1 and PGK2) encoded by two genes have been identified in humans. PGK1 is expressed in all somatic cells, including red blood cells (Willard et al., 1985; McCarrey and Thomas, 1987; Chiarelli et al., 2012), while PGK2 is sperm cell specific (Boer et al., 1987). PGK1 has been implicated in the metabolism of tumor cells (Lay et al., 2000; Hwang et al., 2006; Zieker et al., 2008, 2010; Ai et al., 2011) and also in nuclear DNA replication and repair (Popanda et al., 1998). PGK2 is essential for sperm motility and fertility (Danshina et al., 2010).

In plants, PGKs are involved in not only glycolysis/gluconeogenesis but also in photosynthetic carbon metabolism. Two highly conserved PGK isoforms were initially identified in wheat (*Triticum aestivum*; Longstaff et al., 1989). One of them was located primarily in the cytosol, while the other was plastid localized (Anderson and Advani, 1970). Although the two PGKs could theoretically catalyze both the forward and reverse reactions, it was assumed that the cytosolic isoform is involved in glycolysis and gluconeogenesis, while the plastidial isoform participates, at least in photosynthetic cells, in both the Calvin-Benson cycle and plastidial glycolysis (Anderson et al., 2004). However, this latter assumption has not been thoroughly investigated to date. Subsequently, a second cytosolic PGK isoform from sunflower (*Helianthus annuus*) was cloned (Troncoso-Ponce et al., 2012), and in the Arabidopsis (*Arabidopsis thaliana*) genome, an additional putative PGK isoform with an N-terminal plastid/chloroplast localization signal was identified (Ouibrahim et al., 2014). The presence of two PGKs in the plastid/chloroplast could lead to specialization, so that one of them could be involved in photosynthesis and the other in glycolysis, which seems to be the case of GAPDH isoforms (Anoman et al., 2015). Indeed, a mutant of one of the Arabidopsis plastidial isoforms (At1g56190; *AtPGK2*) has been described as lethal (Myouga et al., 2010; Ouibrahim et al., 2014), which suggests that the two plastidial isoforms are not functionally redundant and likely play different roles in plant metabolism. Moreover, chloroplastic and cytosolic PGK proteins were localized in the nucleus by immunocytolocalization experiments in pea (*Pisum sativum*; Anderson et al., 2004), which is in keeping with the presence of functional nuclear localization signals in the cytosolic PGK (Brice et al., 2004). This fact led to the hypothesis that PGKs are able to act as moonlighting proteins, playing other roles apart from their participation in metabolism. Accordingly, plastidial PGK2 has been shown to play a role in tolerance to abiotic (Liu et al., 2015; Joshi et al., 2016) and biotic (Ouibrahim et al., 2014) stresses. PGK2 has proven to be necessary for watermelon mosaic virus infection (Ouibrahim et al., 2014). Specifically, PGK2 could mediate the transport of viruses to the chloroplast (Lin et al., 2007; Cheng et al., 2013). The in vitro regulation of some PGK isoforms has been studied (Troncoso-Ponce et al., 2012; Morisse et al., 2014). It has been shown that the chloroplastic isoform of *Chlamydomonas reinhardtii* could be light regulated by thioredoxins (Morisse et al., 2014). Furthermore, at the biochemical level, glycolytic PGK activity has been reported to increase in sunflower developing embryos in conjunction with the oil content (Troncoso-Ponce et al., 2009). It has also been shown that PGK and enolase are two of the activities implicated in the differences in oil content between standard and low-oil-content sunflower lines (Troncoso-Ponce et al., 2010). Yet, to date, no genetic or molecular evidence has been found to support the metabolic function of specific PGKs. In this work, we have followed a loss-of-function approach to functionally characterize all the glycolytic and photosynthetic isoforms annotated in the Arabidopsis genome at both the molecular and physiological levels. We unraveled the specific contribution of each isoform to the primary metabolism of aerial parts (AP) and roots and concluded that both glycolytic and photosynthetic isoforms are coregulated to maintain the equilibrium between catabolic and anabolic processes.

## RESULTS

### Expression Analysis and Subcellular Localization of the PGK Family

In The Arabidopsis Information Resource database (http://www.arabidopsis.org), we found three genes encoding putative PGKs: At3g12780, At1g56190, and At1g79550. According to the literature, we named the proteins coded by these genes PGK1, PGK2, and PGK3, respectively. PGK1 displays 91% and 84% amino acid identity with PGK2 and PGK3, respectively, while the amino acid identity between PGK2 and PGK3 is 85%. The three isoforms show 100% identity in all residues

that form the putative catalytic site and the ligand-binding domain (Supplemental Fig. S1A). The cladogram confirmed that PGK1 and PGK2 are more closely related to one another than to PGK3 (Supplemental Fig. S1B). We next assessed the expression patterns of the *PGK* family genes by quantitative real-time (RT)-PCR and by analysis of promoter-GUS fusions in both seedlings and adult plants. *PGK1* was expressed mainly in the leaves, and very poorly in roots, at both seedling and adult stages (Fig. 2, A and B). *PGK2* also was expressed mainly in leaves, especially at the seedling stage, but at the adult stage, its relative expression in roots, siliques, and flowers was higher than that of *PGK1*. By contrast to *PGK1* and *PGK2*, *PGK3* was highly expressed in roots, especially at the seedling stage. At the adult stage, its expression pattern was the most homogenous of all three PGKs, being expressed similarly in all organs studied. These data confirm publicly available microarray expression data (http://bar.utoronto.ca/efp/cgi-bin/efpWeb.cgi). The promoter-GUS analysis revealed a generalized expression of *PGK1* in leaves and cotyledons, especially in guard cells and the surroundings of the vasculature, in petals and sepals, and confirmed the lack of *PGK1* expression in reproductive organs and roots (Fig. 2C; Supplemental Fig. S2). *PGK2* was strongly expressed in leaf veins and margins, in the root vasculature, and in floral organs (pedicel, petals, sepals, and stigma; Fig. 2C; Supplemental Fig. S3). *PGK3* was expressed homogenously in all plant tissues, with a high expression in veins and distal zones of leaves, and all over the roots, siliques, and flowers (Fig. 2C; Supplemental Fig. S4). According to the ChloroP prediction server (http://www.cbs.dtu.dk/services/ChloroP/), both PGK1 and PGK2 harbor an N-terminal plastid/chloroplast localization signal (Emanuelsson et al., 1999). To investigate the subcellular localization of the PGK family proteins, we stably expressed PGK-GFP fusion protein constructs under

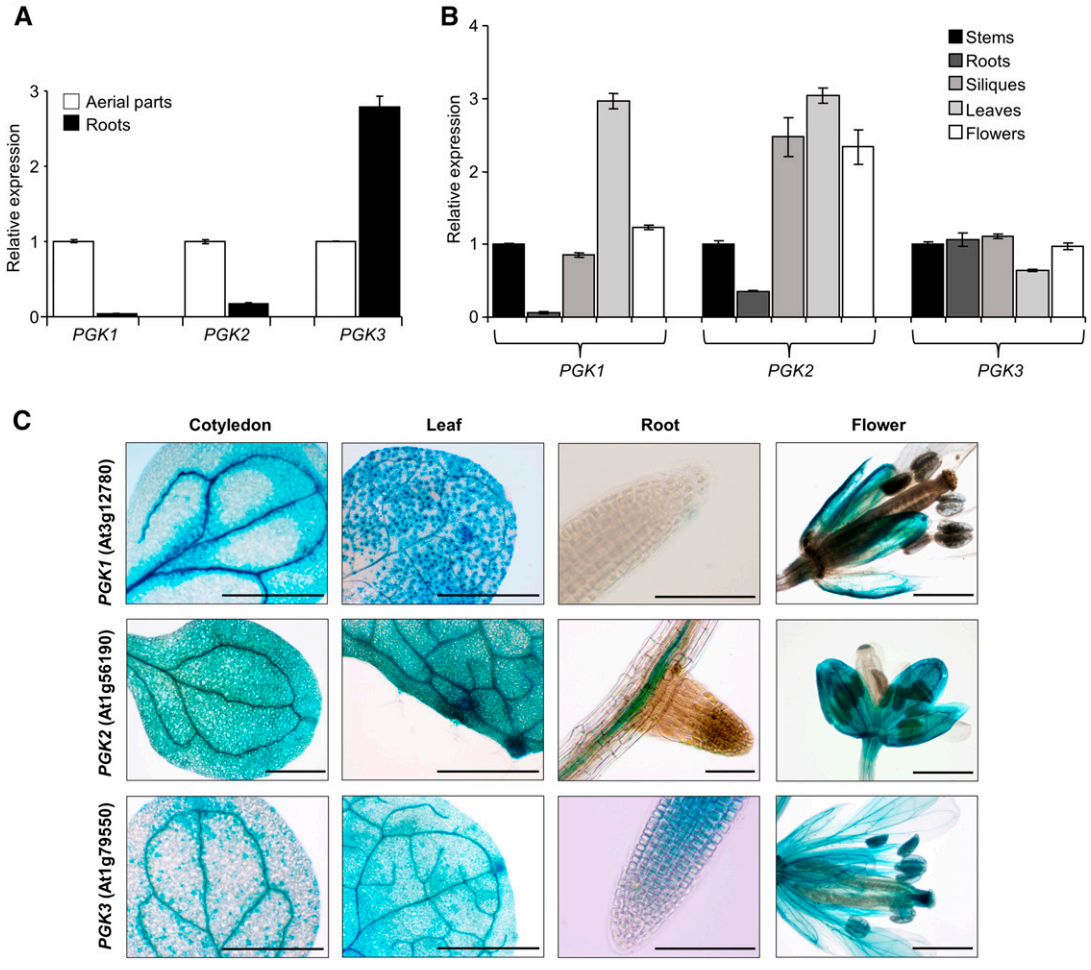


**Figure 2.** Expression analysis of *PGK* family genes. A and B, RT-PCR analysis of *PGKs* in 18-d-old seedlings grown in one-fifth-strength Murashige and Skoog (1/5 MS) medium (A) and in adult plants grown under greenhouse conditions (B). C, *GUS* expression under the control of *PGK1*, *PGK2*, and the *PGK3* promoter in different plant organs. Values in A and B (means ± SE; $n$ = 3 independent biological replicates) are normalized to the expression in the aerial parts (A) or stems (B). Bars in C = 1 mm (cotyledons, leaves, and flowers) and 0.1 mm (roots).

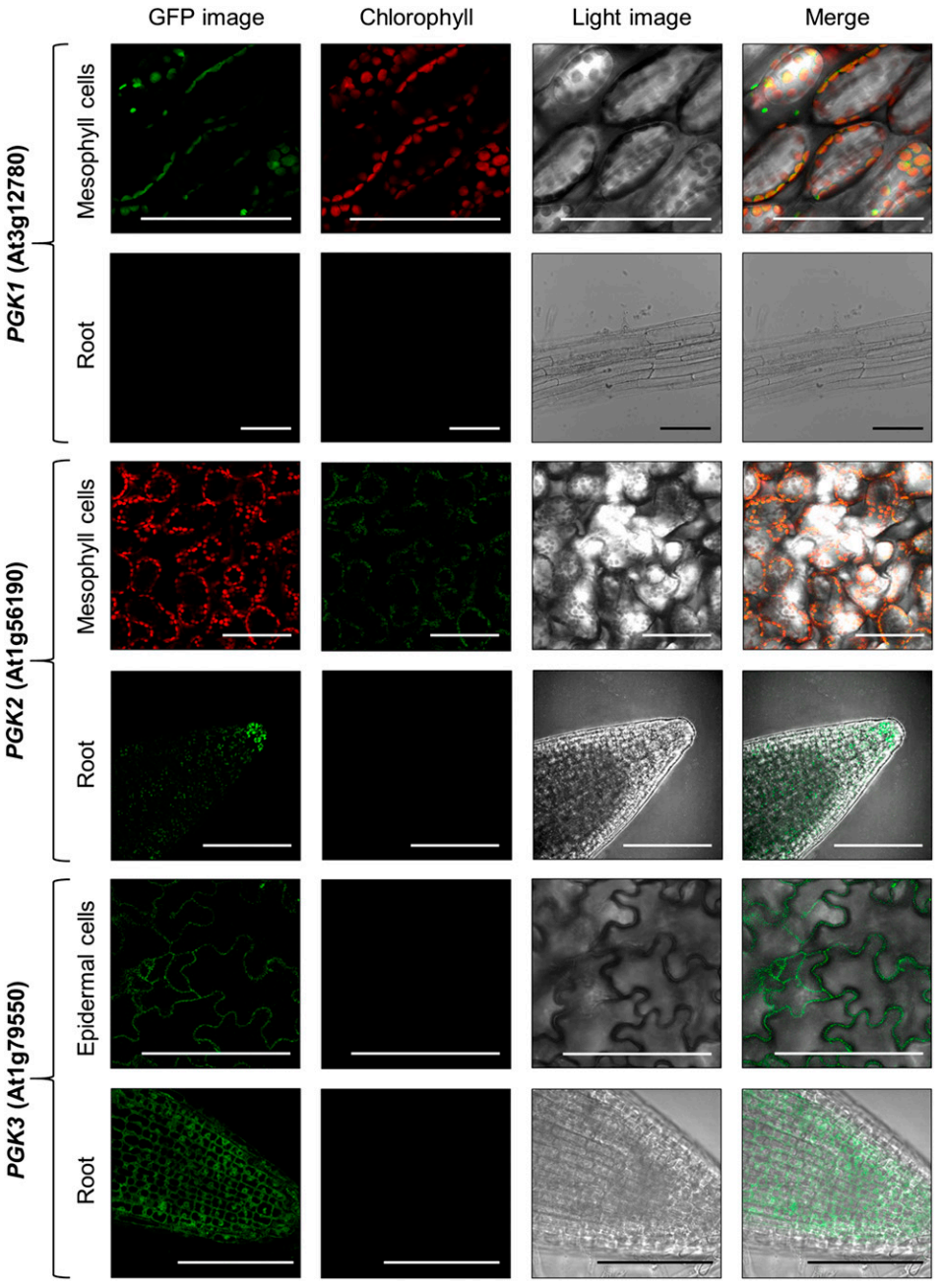


**Figure 3.** Subcellular localization of PGK isoforms by stable expression of PGK-GFP fusion proteins under the control of PGK native promoters. Bars = 100 $\mu$m.

the control of the PGK endogenous promoters in Arabidopsis (*ProPGK1*:*PGK1-GFP*, *ProPGK2*:*PGK2-GFP*, and *ProPGK3*:*PGK3-GFP*). PGK1 was expressed mainly in the cloroplasts of mesophyll cells, and no signal was observed in roots (Fig. 3). PGK2 was expressed in leaf plastids/chloroplasts. In roots, PGK2 was not expressed homogenously but displayed high expression in the columnela plastids. PGK3 was similarly expressed in the cytosol of both root and leaf cells (Fig. 3). PGK3 also could be localized in the nucleus, as confirmed by the nuclear Hoechst marker (Supplemental Fig. S5).

### Phenotypic Characterization of *PGK* Mutants

In order to shed light on the in vivo function of *PGKs*, a loss-of-function approach was followed. T-DNA insertion lines for each *PGK* gene were identified in the databases. The genomic location of the T-DNA insertions was verified by PCR with genomic DNA and sequencing of PCR products (Fig. 4A; Supplemental Table S1). In *pgk1.1* (GK_172A12) and *pgk1.2* (GK_908E11), the T-DNA insertions were located in the 5′ untranslated region (Fig. 4A). In *pgk2.1* (SALK_016097), the T-DNA insertion was located in the

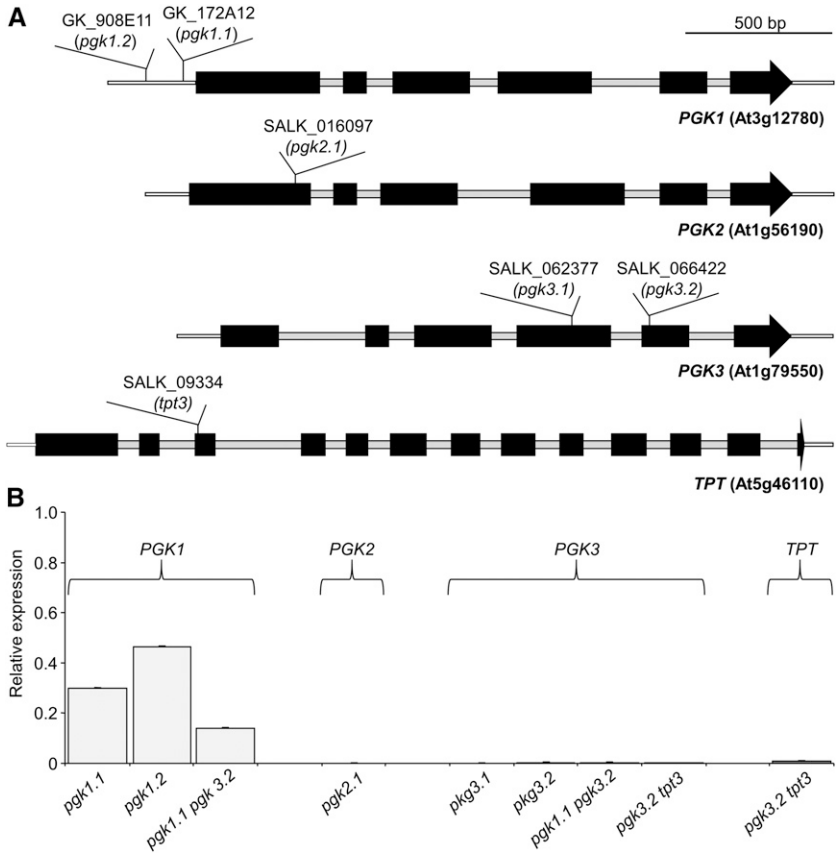


**Figure 4.** Genomic organization and expression analysis of the *PGK* and *TPT* T-DNA mutant lines. A, Black boxes represent exons, and gray lines represent introns. The T-DNA insertion point in each mutant is shown. B, Detection of the *PGK* and *TPT* transcripts in the aerial parts of 18-d-old seedlings of single and double mutants by RT-PCR analysis. Values (means ± SE; $n = 3$ independent biological replicates) are normalized to the expression in the wild type.

first exon. In *pgk3.1* (SALK_062377) and *pgk3.2* (SALK_066422), the T-DNA insertions were located in the fourth and fifth exons, respectively (Fig. 4A). Based on PCR genotyping, the segregation analysis of about 200 seeds from self-fertilized heterozygous plants for *PGK1* or *PGK3* mutant alleles *pgk1.1*, *pgk1.2*, *pgk3.1*, and *pgk3.2* displayed a typical Mendelian ratio of 1:2:1 (homozygous mutant:heterozygous:wild type). RT-PCR analysis indicated that *PGK3* mutants were knockout while both *PGK1* mutants were knockdown (Fig. 4B). The mutant *pgk1.1* showed the lowest *PGK1* expression and was chosen for further analysis (Fig. 4B).

The analysis of *pgk2.1* seedlings from self-fertilized heterozygous plants identified a population of albino individuals when grown on plates with Suc, which were associated with the mutant homozygous genotype (mutant:wild-type phenotype ratio of 1:3). This phenotype could indicate that the homozygous *pgk2.1* individuals are lethal, as observed formerly in two different T-DNA insertion lines (SALK_016097 and SALK_071724; Myouga et al., 2010; Ouibrahim et al., 2014). *PGK2* expression in *pgk2.1* was null (Fig. 4B). However, it was not possible to complement *pgk2.1* with any of the different constructs used herein (a *PGK2* cDNA under the control of the *35S* or native *PGK2* promoter, a genomic *PGK2* sequence), suggesting that there was probably more than one mutation associated with this line. Attempts to separate the albino phenotype from the T-DNA insertion by backcrosses with wild-type individuals were unsuccessful. As a genotype-phenotype correlation was not found, this mutant allele was discarded for further experiments. Instead, *PGK2* down-regulated lines were made using artificial microRNAs (amiRNAs). Fifteen lines overexpressing an amiRNA directed against the *PGK2* in a wild-type background were obtained, and two lines were selected on the basis of having the lowest *PGK2* transcript level (Supplemental Fig. S6A).

Growth parameters were quantified in homozygous mutants at different stages of development in vitro or in greenhouse conditions (Fig. 5). *PGK3* mutants presented a significant reduction in all growth parameters measured as compared with wild-type controls at all growth stages analyzed (Fig. 5, A–D). *pgk1.1* displayed a trend to a reduced growth on plates that was significant in greenhouse conditions, where irradiance was higher (Fig. 5C). To support that the reduction of growth in *pgk1.1* was associated with a lower *PGK1* expression, amiRNA silenced lines were obtained (Supplemental Fig. S6B). The reduced growth of these lines corroborated the relation between *PGK1* expression level and growth (Fig. 5, A–C). The *amiRNA-PGK2* lines displayed milder phenotypes than mutants from other genes, and only one of the two selected lines with

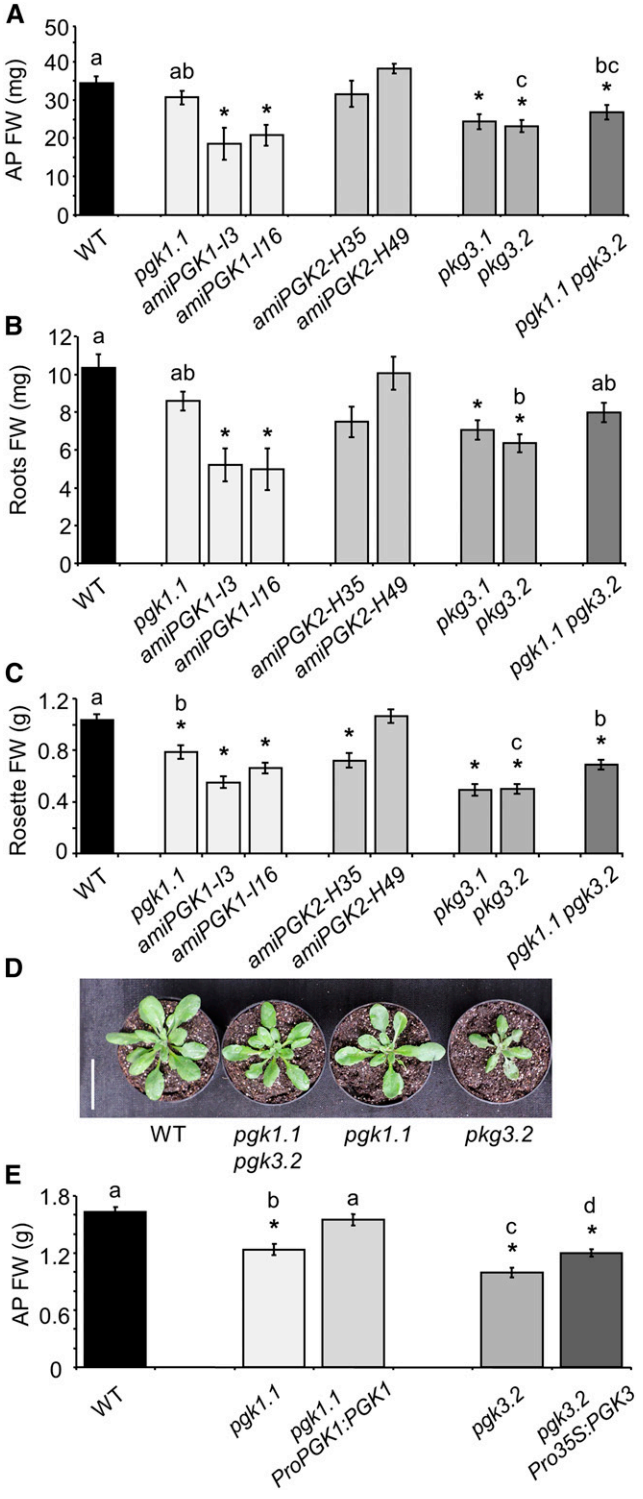


**Figure 5.** A to C, Phenotypical analysis of *PGK* T-DNA mutants and silenced lines grown in 1/5 MS (18-d-old seedlings) or greenhouse conditions (30-d-old plants) as compared with wild-type plants (WT). Seedling AP and root fresh weight (FW) of different lines grown in vertical plates are shown in A and B, respectively. Rosette fresh weight is shown in C. D, Photograph of representative individuals of each line grown in the greenhouse. E, Fresh weight of the AP of mutant and complemented lines grown in the greenhouse. In A to C, Values are means ± SE ($n \geq 36$ plants). In E, data are means of two independent transgenic lines. *, Significantly different as compared with the wild type; different letters indicate significant differences between the wild type and single and double mutants ($P < 0.05$). Bar= 5 cm

the lowest *PGK2* expression level showed a significant reduction of rosette fresh weight as compared with controls (Fig. 5C). No changes in photosynthetic activities were observed in these lines (Supplemental Table S2).

Lower photosynthetic capacity was observed in 20- and 30-d-old *pgk1.1* plants, as inferred from the decreased net photosynthetic rate and the effective and maximum photochemical yield of PSII (Table I). These results, together with the observed plastidial localization of PGK1, would suggest a role of this isoform in the Calvin-Benson cycle. Accordingly, lower starch content was measured in *pgk1.1* plants (Fig. 6A). No differences in photosynthetic parameters were observed in 20-d-old plants of *pgk3.2* in comparison with the wild type (Table I). In this mutant, starch levels were higher than in the wild type. These results, alongside the localization studies, would support the hypothesis that PGK3 is involved in the cytosolic glycolysis. However, in 30-d-old plants, the photosynthetic activity decreased in *pgk3.2*, which suggest that low cytosolic glycolytic activity affects photosynthesis in the long term (Table I).

To further corroborate the genotype-phenotype correlation of *pgk1.1* and *pgk3.2*, we transformed the mutants with a construct carrying the native *PGK1* or *PGK3* cDNA under the control of the endogenous or the *35S* promoter, respectively. We were able to complement the growth phenotypes associated with both the *pgk1.1* and *pgk3.2* mutations (Fig. 5E). Accordingly, the photosynthetic parameters were completely or partially recovered in *pgk1.1* and *pgk3.2* complemented lines (Table I).

### Metabolomics Profile of Down-Regulated *PGK* Lines

To understand the contribution of the PGKs to the primary metabolism, we studied the metabolomics profile of the *PGK* mutants. A clearly altered metabolite content in the AP and roots of mutants was observed (Fig. 7; Supplemental Table S3).

In the *pgk1.1* AP, the most important changes were found in the amino acid pool. Many amino acids (threonic acid, Ala, Asp, and Pro) increased by more than 40% as compared with the wild type (Fig. 7; Supplemental Table S3). Sugars were not so strongly affected, and none of them varied by more than 40% as compared with the wild type, although Glc and Suc increased by 29% and 24%, respectively. In roots, the pattern of metabolite modifications differed from that obtained in the AP, and the sugar levels were especially affected (Fig. 7; Supplemental Table S4), with all the quantified sugars and sugar derivatives, with the exception of glyceraldehyde-3-phosphate, being increased significantly. Quantitatively, the most striking

**Table I.** *Photosynthetic parameters in* PGK *single and double mutants and in complemented lines.*

Photosynthetic rate ($A_N$; $\mu$mol $m^{-2}$ $s^{-1}$) and effective (PhiPS2) and maximum photochemical yield of PSII ($F_v/F_m$) in 20- and 30-day-old plants are shown. Each value is the mean ± SE of 10 independent determinations. For each growth stage, different letters indicate significant differences between groups ($P < 0.05$).

| Sample | Age | Genotype | $A_N$ | PhiPS2 | $F_v/F_m$ |
|---|---|---|---|---|---|
| Mutants | 20 d | Wild type | 7.0 ± 0.348 a | 0.139 ± 0.004 a,b | 0.769 ± 0.003 a |
| | | *pgk1.1* | 4.7 ± 0.332 b | 0.112 ± 0.004 c | 0.745 ± 0.008 b |
| | | *pgk3.2* | 7.5 ± 0.408 a | 0.151 ± 0.007 a | 0.766 ± 0.006 a |
| | | *pgk1.1 pgk3.2* | 5.0 ± 0.365 b | 0.128 ± 0.006 b | 0.768 ± 0.007 a |
| | 30 d | Wild type | 9.1 ± 0.295 a | 0.174 ± 0.004 a | 0.769 ± 0.002 a |
| | | *pgk1.1* | 6.2 ± 0.115 c | 0.130 ± 0.004 c | 0.758 ± 0.004 b |
| | | *pgk3.2* | 7.5 ± 0.276 b | 0.160 ± 0.004 b | 0.752 ± 0.004 b |
| | | *pgk1.1 pgk3.2* | 7.0 ± 0.222 b | 0.140 ± 0.004 c | 0.777 ± 0.001 a |
| Complemented lines | 20 d | Wild type | 9.0 ± 0.606 a | 0.115 ± 0.005 a | 0.778 ± 0.003 a |
| | | *pgk1.1* | 5.1 ± 0.502 c | 0.077 ± 0.006 c | 0.748 ± 0.005 b |
| | | *pgk1.1 ProPGK1:PGK1GFP-L3* | 7.0 ± 0.257 b | 0.089 ± 0.004 b,c | 0.753 ± 0.005 b |
| | | *pgk1.1 ProPGK1:PGK1GFP-L15* | 7.7 ± 0.494 a,b | 0.101 ± 0.006 a,b | 0.760 ± 0.003 b |
| | 30 d | Wild type | 8.6 ± 0.128 a | 0.140 ± 0.004 a | 0.759 ± 0.007 a |
| | | *pgk3.2* | 4.8 ± 0.590 c | 0.122 ± 0.006 b | 0.754 ± 0.008 a |
| | | *pgk3.2 Pro-35S:PGK3-GFP-L1* | 7.2 ± 0.099 b | 0.141 ± 0.003 a | 0.761 ± 0.006 a |
| | | *pgk3.2 Pro-35S:PGK3-GFP-L11* | 7.0 ± 0.236 b | 0.151 ± 0.080 a | 0.743 ± 0.152 a |

changes were those in the levels of Fru (103% increase) and Glc (71% increase).

The *pgk3.2* AP showed a general increase in amino acids and sugar levels (Fig. 7; Supplemental Table S3). Of the 21 amino acids detected, the increases were significant in seven, while the decreases were significant only in three. Some, such as Gln and *O*-acetyl Ser, increased by more than 40%. In addition, increases were observed in more than half of the quantified sugars, and the increases in Fru (up to 164%) and Glc (113%) levels were particularly noteworthy. In the *pgk3.2* roots, the most prominent changes were observed in certain organic acids (e.g. succinic and citric, which increased 52% and 108%, respectively; Fig. 7; Supplemental Table S4). As for soluble sugars, the increase was higher than that observed in the AP, especially the increases in Glc (167%) and Fru (287%). Similar changes in the *pgk3.2* AP and roots also were found in the glyceric and phosphoric acid contents, which decreased in both organs.

Significant changes were found in the *amiRNA-PGK2* lines, but they were generally less dramatic than in the other studied mutants (Fig. 7; Supplemental Tables S3 and S4). In the *amiRNA-PGK2* AP, there was a general trend toward a decrease in the metabolite content, but only raffinose was reduced by more than 40%. In roots, an increasing trend was noted in metabolite content, but, once again, changes were not as drastic as in the other mutant lines (approximately 10% different from wild-type levels).

### The *PGK1* and *PGK3* Double Mutation Compensates the Growth Defects and Metabolic Disorders of Single Mutants

Transcriptomics data provided in the databases (http://bar.utoronto.ca/efp/cgi-bin/efpWeb.cgi) and our own RNA sequencing (RNA-seq) data indicate that *PGK1* is the most abundant PGK transcript in Arabidopsis leaves (with counts in the AP as follows: *PGK1*, 945; *PGK2*, 118; and *PGK3*, 102). PGK cytosolic activity accounts for 5% to 10% of total PGK activity in barley (*Hordeum vulgare*) and spinach (*Spinacia oleracea*), while chloroplastic activities account for 90% to 95% (Köpke-Secundo et al., 1990; McMorrow and Bradbeer, 1990). These activity data well agree with the transcript abundance of PGK isoforms in the Arabidopsis AP.

We observed a significant reduction in PGK total activity in the AP of 20-d-old *pgk1.1* seedlings and a nonsignificant trend to a reduction in *pgk3.2* (Fig. 6B). Since *PGK1* is the most abundant transcript in the AP, changes in the activity of other isoforms could be masked or be difficult to detect in this organ. However, in roots, where *PGK3* transcripts are the most abundant (with counts in the roots as follows: *PGK1*, 46; *PGK2*, 62; and *PGK3*, 262), a reduction of about 75% of total PGK activity was observed in *pgk3.2*, while no activity changes were observed in *pgk1.1* as compared with the wild type. Since *pkg3.2* is knockout, the remaining 25% of PGK activity measured in the mutant roots could be due to both PGK1 and PGK2 isoforms. There were no differences in *amiPGK2* activity in either AP or roots, which may imply that the silencing is not absolute and/or that it is a global minority isoform in both organs, as evidenced by the transcriptomics data.

In 30-d-old plants, a significant reduction in the AP PGK activity was observed in both *pgk1.1* and *pgk3.2*. Besides, this reduction was more marked in 30-d-old than in 20-d-old *pgk1.1* plants as compared with controls. Differences in total PGK activity in the mutant at seedling (20 d old) and adult (30 d old) stages could be related to changes in PGK gene expression. For this reason, we studied the *PGK* family gene expression in the different mutant backgrounds at different

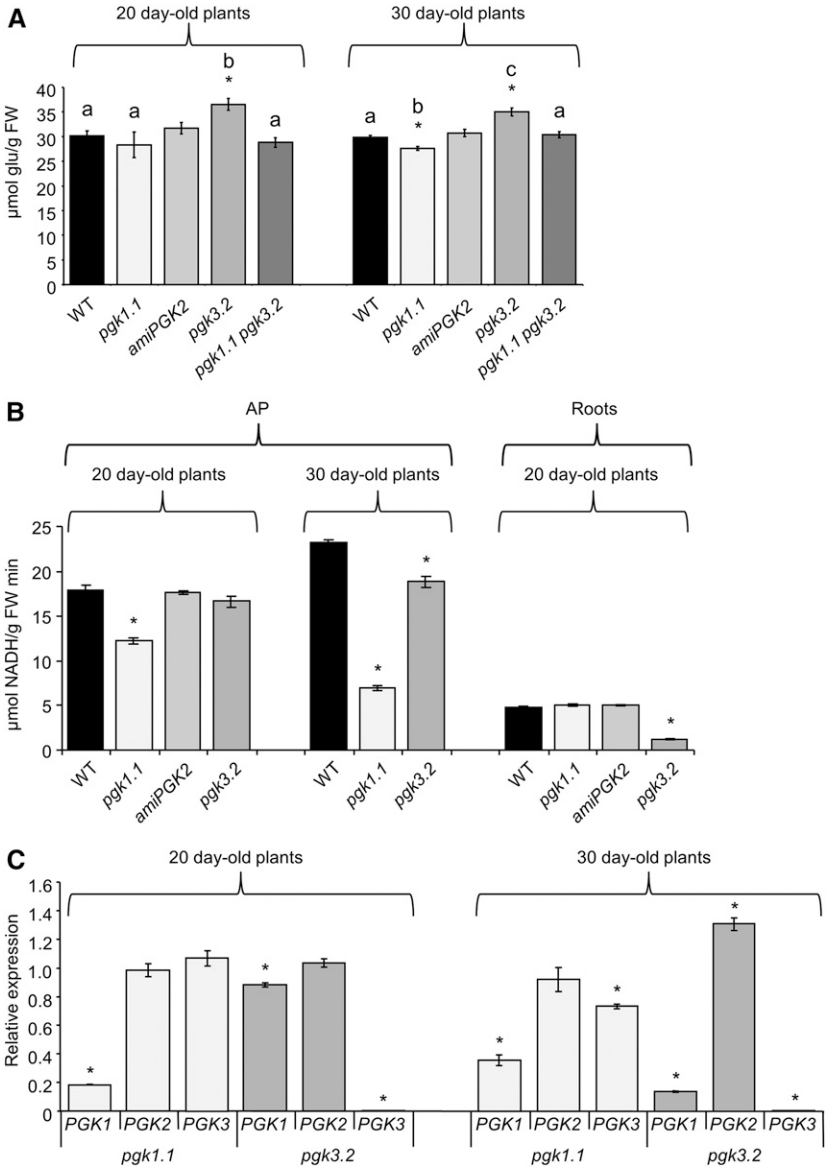


**Figure 6.** Biochemical and molecular analyses of *PGK* mutant and silenced lines (amiRNA lines) as compared with wild-type plants (WT). A to C show starch content, PGK activity, and RT-PCR analysis of PGKs in the AP of 20- and 30-d-old plants grown in the greenhouse. In B, PGK activity also was measured in 20-d-old roots grown on plates. Values are means ± SE ($n \geq 30$ plants). In A and B, data from the silenced lines are means of individuals from two independent transgenic lines. *, Significantly different as compared with the wild type; different letters indicate significant differences between groups ($P < 0.05$). FW, Fresh weight.

developmental stages (Fig. 6C). At the seedling stage only, *PGK1* expression was reduced slightly in *pgk3.2*. However, in adult plants, *PGK1* and *PGK3* expression was dramatically down-regulated in *pgk3.2* and *pgk1.1*, respectively. The reduction in photosynthetic activity observed in 30-d-old *pgk3.2* (Table I) could be associated with the repression of *PGK1* in the mutant at this developmental stage.

All these results could indicate that PGK expression is regulated at the transcriptional level to adjust metabolism. To corroborate this hypothesis, a double mutant of *pgk1.1* and *pgk3.2* was generated and subsequently studied. *pgk1.1 pgk3.2* did not show more dramatic phenotypes as compared with single mutants. On the contrary, the *pgk1.1 pgk3.2* growth phenotype was less severe than that of *pgk3.2* (Fig. 5, C and D), and the starch levels and photosynthetic activities were less affected as compared with *pgk1.1* (Fig. 6A; Table I). Double mutants improved their growth and photosynthetic activities as compared with single mutants as plants were getting older, suggesting a long-term compensatory effect of the double mutation (Fig. 5, A–D; Table I).

The metabolite analysis confirmed a compensatory effect of the double mutation (Fig. 7; Supplemental Tables S3 and S4). For instance, some metabolites, such as Ala and Pro, increased in the *pgk1.1* AP by more than 40% compared with the wild type but did not differ significantly in the *pgk3.2* AP. In *pgk1.1 pgk3.2*, the AP contents of such metabolites did not differ significantly from those in the wild type either (Fig. 7; Supplemental Table S3). In the *pgk3.2* AP, the metabolites that varied

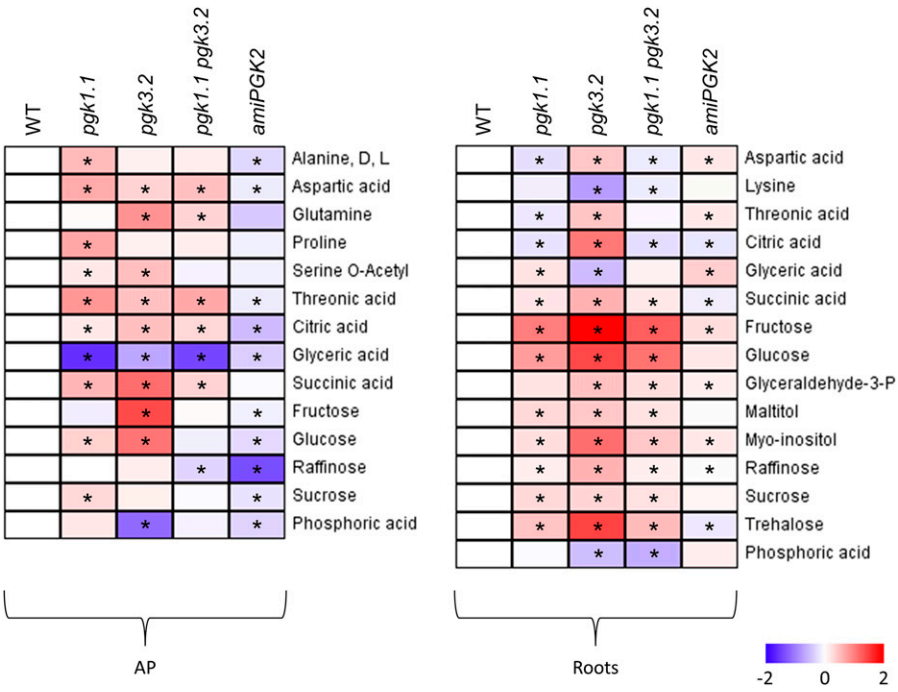


**Figure 7.** Most relevant changes in the metabolite content of AP and roots of 21-d-old *pgk* mutants and silenced lines grown on vertical plates as compared with the wild type (WT). $Log_2$ values of the relative metabolic contents are presented as a heat map. *, Significant differences between the mutant and the wild type ($P < 0.05$). Detailed results of the assay are presented in Supplemental Tables S3 and S4.

more than 40% but whose content did not differ with respect to wild type in *pgk1.1* were Gln (80%) and Fru (164%; Fig. 7; Supplemental Table S3). In *pgk1.1 pgk3.2*, the Gln content was significantly higher than in the control, but decreased to 30%, whereas the Fru content did not show significant differences. Finally, the contents of those metabolites that changed in the same direction in both single mutants (succinic acid, Asp, *O*-acetyl-Ser, citric acid, and Glc) were not superior in the double mutant to those of the single mutants but, rather, were intermediate or more similar to the wild type. The trend described above for the AP was additionally observed in roots (Fig. 7; Supplemental Table S4).

### Blocking the Flux of 3-PGA between the Plastid and the Cytosol Accentuates the *pgk3.1* Phenotypes

PGK3 should provide the 3-PGA needed for the essential reactions of the glycolytic cytosolic pathway. In spite of PGK3 being the sole cytosolic PGK isoform, the knockout *pgk3.2* was viable. The relative 3-PGA level was not reduced but increased in *pgk3.2* plants compared with the wild type (Fig. 8A). We postulate that some of the 3-PGA needed for respiration could be provided by plastidial glycolysis and be transported to the cytosol by the triose phosphate transporter (TPT), the main carbon transporter in the AP. To investigate this hypothesis, we interrupted the metabolite communication between the cytosol and the plastids by generating a double knockout mutant of *pgk3.2* and TPT (*tpt3*; Fig. 4A).

The *pgk3.2 tpt3* double knockout mutant showed a more dramatic growth phenotype than the single mutants, indicating an additive effect of the mutations (Fig. 8B). Accordingly, the starch level in the AP of *pgk3.2 tpt3* was even higher than in *tpt3* (Fig. 8C). The metabolomics analysis of the *pgk3.2 tpt3* AP indicated that there was a general increase in amino acid content as observed in *pgk3.2* (Fig. 8D; Supplemental Table S5). It is worth mentioning that Ser and its derivatives (Met and *O*-acetyl-Ser) also increased, which could indicate an activation of the plastidial phosphorylated pathway of Ser biosynthesis. When amino acids increased in both single mutants, an additive effect was always observed in the double mutants. Interestingly, the glyceric and phosphoric acid contents, which decreased dramatically in *pgk3.2*, increased in *tpt3*. In *pgk3.2 tpt3*, these metabolites displayed an intermediate phenotype. Sugar levels (Glc, Man, and Fru) increased in *pgk3.2* but were decreased in *tpt3*, displaying intermediate values in *pgk3.2 tpt3*. Once again, when sugar trends were similar in both single mutants, the change became more marked in *pgk3.2 tpt3*. For example, galactinol, myoinositol, Xyl, and trehalose, which increased in both single mutants, were further increased in *pgk3.2 tpt3*. Thus, the metabolomics analysis fully corroborated the additive effect of the double mutation.

## DISCUSSION

### Functions of the PGK Isoforms and Impact in Plant Development

The study of the expression patterns of PGK family genes, as well as their intracellular localization, provided important information concerning their function

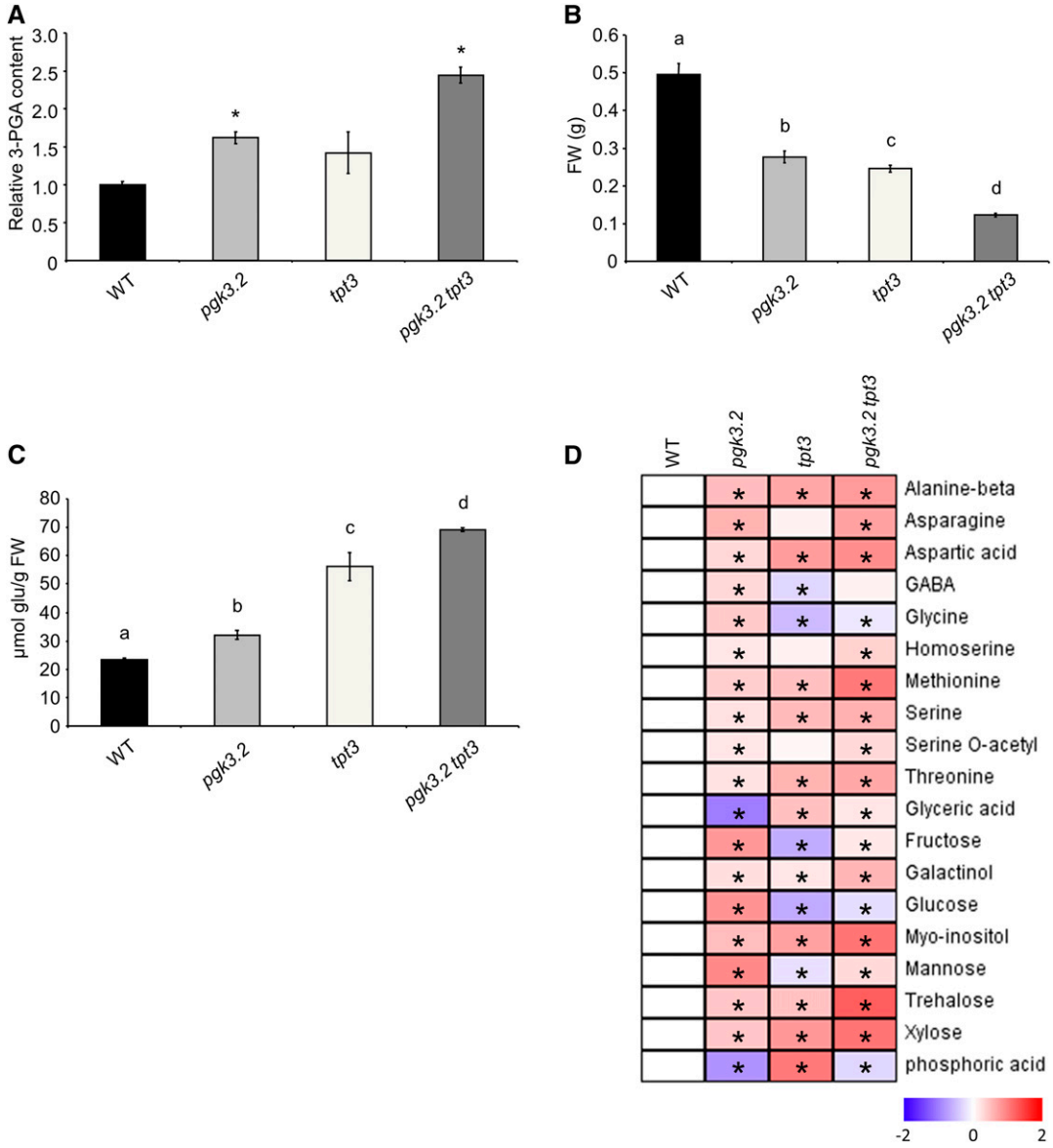


**Figure 8.** Phenotypical, biochemical, and molecular analyses of the *pgk3.2 tpt3* mutant as compared with single mutants (*pgk3.2* and *tpt3*) and the wild type (WT). A, Relative 3-PGA content in the AP of 25-d-old plants grown in the greenhouse normalized to the mean content of the wild type ($34 \pm 1$ $\mu g\, g^{-1}$ fresh weight). B and C, Rosette fresh weight (FW) and starch content of the AP of 25-d-old plants grown in the greenhouse. D, Most relevant changes in the metabolite content of AP of 19-d-old *pgk3.2 tpt3* lines grown on vertical plates as compared with single mutants and the wild type. $Log_2$ values of the relative metabolic contents are presented as a heat map. Detailed results of the assay are presented in Supplemental Table S5. *, Significantly different as compared with the wild type; different letters indicate significant differences between groups ($P < 0.05$).

in Arabidopsis. Both PGK1 and PGK2 are plastid localized, while PGK3 is localized in both the cytosol and the nucleus. The nuclear localization of PGK3 corroborates previous findings in pea (Anderson et al., 2004), which could indicate that this enzyme not only participates in metabolism but also performs additional functions, as demonstrated previously in mammals. *PGK1* is expressed almost exclusively in photosynthetic tissues, and *PGK3* is quite uniformly expressed in all organs. The expression studies, along with the results obtained in the metabolomics and photosynthetic analyses of the different lines (i.e. lower levels of starch and photosynthetic activities in *pgk1.1*) clearly indicate that PGK1 is a photosynthetic isoform, whereas PGK3 is the cytosolic glycolytic isoform.

The low values of the maximum quantum efficiency of PSII in *pgk1.1* suggest the existence of a photoinhibition or photosynthetic damage phenomenon. This negative effect could be related to a reduced PGK1 activity in this mutant. PGK consumes most of the ATP

required in the Calvin-Benson cycle, so its low activity would limit the regeneration of electron acceptors required for the operation of the photosynthetic electron transport chain. The smaller *pgk1.1* size may be related to their lower photosynthetic capacity and/or damage caused by photoinhibition. The negative effect on mutant growth was observed more clearly under greenhouse conditions, where the light intensity is higher than in growth chambers. In the greenhouse, the greater photosynthetic capacity of the wild type and/or its lesser photoinhibition could accentuate the growth differences between the two lines.

*pgk3.2* showed the more dramatic reduction in growth of all the single mutants characterized here. This may be related to the mutant's incapacity to metabolize carbohydrates for growth, since the starch and sugar levels in this mutant were higher than in the wild type. Thirty-day-old *pgk3.2* displayed symptoms of photoinhibition and a dramatic reduction of *PGK1* expression along with a reduction in photosynthetic activity. The high levels of carbohydrates could have a negative feedback effect on the expression of photosynthetic genes (Paul and Pellny, 2003; Smith and Stitt, 2007; Stitt et al., 2010; McCormick and Kruger, 2015) and, thus, a general inhibition of photosynthesis.

PGK2 was plastid localized and is most probably a glycolytic isoform. Yet, the high *PGK2* expression in leaves raises the question of additional functions in photosynthetic tissues, especially when compared with the low expression of the plastidial glycolytic isoforms of GAPDH in this organ (Muñoz-Bertomeu et al., 2009). Phylogenetic studies of plant PGKs indicate that photosynthetic and glycolytic isoenzymes have a common origin and come from an ancestral eubacteria gene that duplicated and replaced the preexisting eukaryotic gene (Brinkmann and Martin, 1996; Archibald and Keeling, 2003). This situation contrasts with that of the GAPDHs, where the glycolytic isoforms have a eukaryotic origin (Petersen et al., 2003) while the photosynthetic enzymes are prokaryotic in nature (Shih et al., 1986). The bacterial origin of both glycolytic and photosynthetic PGKs could be relevant to both the enzyme activity and regulation and could be related to a greater versatility of these enzyme isoforms. While the Arabidopsis genome has five plastidial and two cytoplasmic GAPDH isoforms, PGK has only one cytosolic and two plastidial isoforms, which indicates a greater degree of specialization in the GAPDH than in the PGK family. A partially redundant function of PGK2 in photosynthesis could explain the high level of gene expression in leaves. However, the *amiRNA-PGK2* lines did not have any effect either on the photosynthetic activity or on the starch content, which renders this hypothesis difficult to prove.

In spite of the possible lethal phenotype of *pgk2.1* (Myouga et al., 2010; Ouibrahim et al., 2014; this study), the *amiRNA-PGK2* lines displayed weaker metabolite changes than the other mutants (Fig. 6). This suggests that either *pgk2.1* is not lethal or that silenced lines have residual levels of PGK2 activity that are sufficient to maintain them. There are other examples of enzymes whose insertional mutants are lethal and whose silenced lines are viable (Cascales-Miñana et al., 2013). This fact reinforces the idea that low transcription levels in amiRNA lines may mask the more dramatic phenotypes observed in knockout mutants; thus, other levels of enzyme posttranscriptional and/or posttranslational regulation (regulation by substrates and other interacting proteins, enzyme biosynthesis turnover) may compensate for the low transcription level. Hence, a silencing strategy may be of limited use for metabolic enzymes. In any case, due to the lack of phenotypic complementation of *pgk2.1*, we cannot rule out that other closely linked mutations may be partly responsible for the observed lethal phenotype of this mutant.

### PGK1 and PGK3 Are Transcriptionally Coregulated to Adjust Metabolism

We found a correlation between PGK gene expression and enzyme activities, which indicates that transcription is an important mechanism of PGK regulation. The importance of transcriptional regulation for PGKs may be related to their bacterial origin and could be different from other metabolic enzymes of eukaryotic origin.

Since *pgk1.1* and *pgk3.2* single mutants displayed reduced growth, we expected this reduction to be even more drastic in the double mutant, as both photosynthetic and glycolytic activities were affected. However, contrary to our expectations, *pgk1.1 pgk3.2* was bigger than *pgk3.2* and displayed an intermediate phenotype between the two single mutants in all measured biochemical and physiological parameters (metabolite contents and photosynthetic activity). These results rule out an additive effect of the double mutation and point rather toward a compensatory effect that could be related to the coregulated *PGK* expression in the single mutants. Thus, *PGK3* expression is repressed in *pgk1.1* in late development stages. Therefore, the reduced PGK activity in this mutant compared with earlier stages might be related to *PGK3* repression, at least in part. The repression of genes involved in sugar catabolism also has been observed in mutants with a low starch content and has been associated with an adaptive response to avoid reserve depletion (Bläsing et al., 2005; Smith and Stitt, 2007).

Furthermore, the reduced PGK activity found in the AP of *pgk3.2* adult plants could be due in part to *PGK1* repression. This repression would avoid the accumulation of carbohydrates in *pgk3.2*, which could have an inhibitory effect on the photosynthetic activity and, thus, ultimately on growth. Our results indicate that, when the glycolysis is limited, the plant tends to readjust the rate of photosynthesis to compensate for the effects caused by the accumulation of carbohydrates, and vice versa. Therefore, reduced photosynthetic activity in the double mutant in early stages would avoid the accumulation of excess sugars as a result of a

diminished glycolytic activity, which has a beneficial effect on the long-term growth of the double mutant as compared with the single mutants.

### PGK3 Activity Is Bypassed in *pgk3* Metabolism

Since metabolism is a complex and dynamic process, it is difficult to predict the metabolite changes associated with the lack of a certain enzyme activity, especially if the same activity is displayed by different isoforms and in distinct compartments. PGK3 should be the main provider of cytosolic 3-PGA for the downstream reactions of glycolysis and, thus, for respiratory activity. Lack of PGK3 activity was associated with an increase in soluble sugar (mainly Glc and Fru) and starch. These increases could be caused by a reduced glycolytic activity that, in turn, slows down plant growth. However, total 3-PGA content, the product of the PGK3 activity, increased in *pgk3.2*. This could indicate that more 3-PGA is generated in *pgk3.2* by other reactions (e.g. through higher photosynthetic activity). However, this was not always the case, since both photosynthetic activity and PGK1 expression were reduced in the adult *pgk3.2* plants in which 3-PGA was measured. Another possible route to increase 3-PGA availability is via the plastidial glycolytic pathway, which, as the increased *PGK2* expression suggests, could have been more active in *pgk3.2*. In the wild-type AP, the triose phosphates are transported from the plastid to the cytosol through the TPT (Fig. 1). We hypothesized that, in *pgk3.2*, PGK2 activity is increased to produce more 3-PGA in the plastid to bypass the PGK3 reaction, which is then transported to the cytosol through the TPT (Fig. 1). Once in the cytosol, 3-PGA could complete glycolysis in order to fuel the tricarboxylic acid cycle when necessary. The increased plastidial glycolytic activity hypothesis also could be applicable to heterotrophic plastids. In root plastids, where TPT activity is absent, 3-PGA can be potentially converted into PEP by phosphoglycerate mutase and enolase (Prabhakar et al., 2010; Flores-Tornero et al., 2017). PEP could be the metabolite transported from the plastid to complete glycolysis in the cytosol. Indeed, it has been postulated that the PEP/inorganic phosphate translocator acts as a net importer of PEP into the chloroplast but as a net exporter in root plastids (Staehr et al., 2014) and probably in plastids from other nonphotosynthetic tissues such as embryos (Flores-Tornero et al., 2017).

The drastic phenotype of *pgk3.2 tpt3* would suggest that the TPT activity could, at least in part, alleviate the PGK3 deficiency. In this double mutant, the 3-PGA formed by photosynthesis or plastidial glycolysis in the AP could not be exported to the cytosol and would accumulate mainly as starch, as it does in the *tpt3* single mutant. Besides, the measured increases in Ser and derivatives (Met and *O*-acetyl-Ser), which were already apparent in *tpt3*, could indicate an activation of the plastidial phosphorylated pathway of Ser biosynthesis to divert part of the 3-PGA flux toward Ser synthesis.

Since *pgk3.2 tpt3* is a double knockout mutant that is still viable, there must be other mechanisms able to supply the essential 3-PGA to the cytosol in the mutant AP. These other possible mechanisms could include the inefficient 3-PGA transport through other chloroplast membrane transporters of the phosphate translocator family, such as Glc or xylulose-5-phosphate translocators (Fischer and Weber, 2002), or the involvement of the nonphosphorylating cytosolic GAPDH, which produces 3-PGA from glyceraldehyde-3-phosphate, bypassing the PGK3 reaction (Rius et al., 2006). These mechanisms, while inefficient, may be sufficient to maintain the mutant's viability.

Evaluation of the metabolomics data from different lines can help to find those changes in metabolite levels that can corroborate the above-postulated hypotheses and establish the connections between different metabolic pathways. Several metabolites changed in the opposite direction in the *pgk3.2* and *tpt3* single mutants, including Glc, Fru, and glycerate. As mentioned previously, the accumulation of Glc, Fru, and starch in *pgk3.2* may be caused by the impairment of their metabolism via glycolysis. In *tpt3*, the low levels of soluble sugars most likely reflect the inhibition of triose phosphate transport to the cytosol and, as such, a restricted substrate supply in support of their formation. Carbohydrates thus instead accumulate in the form of starch, a phenomenon that was also observed in *pgk3.2 tpt3*. Moreover, glyceric acid decreased in *pgk3.2*, increased in *tpt3*, and presented an intermediate value in the double mutant. These reverse changes between *pgk3.2* and *tpt3* could be related to the strategy in *pgk3.2* to redirect the glycolytic flux toward the plastid. Low glyceric acid levels in the AP could be the result of the conversion of this metabolite into 3-PGA by the plastidial glycerate kinase to be transported to the cytosol through TPT (Fig. 1). Interestingly, the phosphoric acid content also decreased dramatically in the *pgk3.2* AP, but it increased in *tpt3*. Given that it correlated with the inorganic phosphate levels, the low phosphoric acid levels in the *pgk3.2* AP may be indicative of the high 3-PGA-inorganic phosphate exchange rate, which, by contrast, is disrupted in *tpt3*.

## CONCLUSION

Our results provide new insights into the functions of PGK isoforms and how they are regulated. The expression studies, along with the biochemical and physiological characterization, demonstrate that PGK1 is the photosynthetic isoform, while PGK2 is most probably involved in plastid glycolysis. PGK3 would be the cytosolic glycolytic isoform.

The study of the double mutant supports both the complexity and the plasticity of the primary metabolic network. Here, it is emphasized that imbalances of photosynthetic metabolism tend to be corrected by the

regulation of the glycolytic routes and vice versa. Therefore, the results obtained in this work support that plastidial and cytosolic metabolism are intimately connected and that regulatory mechanisms exist that tend to maintain the balance between catabolic and anabolic reactions in the central carbon metabolism of plants.

## MATERIALS AND METHODS

### Plant Material and Growth Conditions

Arabidopsis (*Arabidopsis thaliana*) seeds (ecotype Columbia-0) were supplied by the European Arabidopsis Stock Center (Scholl et al., 2000). Seeds were sterilized and sown on 0.8% (w/v) agar plates containing 1/5 MS medium with Gamborg vitamins buffered with 0.9 g $L^{-1}$ MES (adjusted to pH 5.7 with Tris). After a 4-d treatment at 4°C, plates were vertically placed in a growth chamber (IBERCEX; V350) at 22°C under a 16-h-day/8-h-night photoperiod at 100 $\mu$mol $m^{-2}$ $s^{-1}$. To select the transgenic plants, one-half-strength MS plates supplemented with 0.5% (w/v) Suc and appropriate selection markers were used. Some seeds also were grown under greenhouse conditions in pots filled with a 1:1 (v/v) mixture of vermiculite and fertilized peat (KEKILA 50/50; Kekkilä Iberia) irrigated with demineralized water as required. Trays were placed in a cold chamber (4°C) and were placed under the greenhouse staging after 4 d. Growth conditions consisted of 16 h of light, 50% to 70% (v/v) relative humidity, and an average temperature of 24°C during the daytime and 17°C during the night. Whenever necessary, these conditions were supplied with artificial light from sodium and mercury vapor lamps. For analyses, 18- to 30-d-old prebolting material from plates or pots was harvested and separated into AP (including leaves and cotyledons) and roots. Unless stated otherwise, the material was sampled at the middle of the light period.

### Primers

All primers used in this work are listed in Supplemental Table S6.

### Mutant Isolation and Characterization

The mutant alleles of *PGK1* (At3g12780), *PGK2* (At1g56190), *PGK3* (At1g79550), and *TPT* (At5g46110) were identified in the SIGnAL Collection database at the Salk Institute (Alonso et al., 2003): GK_172A12 and GK_908E11 for *PGK1*, SALK_016097 for *PGK2*, SALK_062377 and SALK_066422 for *PGK3*, and SALK_09334 for *TPT*. Mutants were identified by PCR genotyping using gene-specific primers and left border primers of the T-DNA insertion (Supplemental Table S6). The T-DNA insertions were confirmed by sequencing the fragment amplified by the T-DNA internal primers and gene-specific primers (Supplemental Table S6).

### Cloning and Plant Transformation

Standard methods were used to make the gene constructs (Sambrook and Russell, 2001). For gene promoter-GUS fusions, genomic DNA was PCR amplified using primers At3g12780PromHind3F and At3g12780PromSpeR for the *PGK1* promoter (1,508 bp), At1g56190PromNcoIR and At1g56190PromXbaIF for the *PGK2* promoter (1,466 bp), and At1g79550PromSpeIR and At1g79550-PromHind3F for the *PGK3* promoter (1,284 bp). Plasmid pCAMBIA1303 was used to fuse the promoter fragments to the GUS gene using the sites indicated in the respective primer names.

For promoter-PGK-GFP fusions, PGK cDNAs were PCR amplified with the following primers: At3g12780GFP-F and At3g12780GFP-R for *PGK1*, At1g56190GFP-F and At1g56190GFP-R for *PGK2*, and At1g79550GFP-F and At1g79550GFP-R for *PGK3*. PCR products were cloned in the pCR8/GW/TOPO plasmid (Invitrogen). These cDNAs were subcloned in the plasmid pMDC83 under the control of the *35S* promoter (Curtis and Grossniklaus, 2003) using Gateway technology with Clonase II (Invitrogen). The pMDC83 plasmids allowed us to clone *PGK* cDNAs in frame with a GFP cDNA at the C-terminal position (PGK1-GFP, PGK2-GFP, and PGK3-GFP). Promoter regions of PGKs cloned previously in pCAMBIA1303 were PCR amplified to introduce restriction sites (primers At3g12780PmeIProF and At3g12780PromSpeR introduced *Pme*I and *Spe*I restriction sites into the *PGK1* promoter; primers At1g56190F-ProPmeI and At1g56190RevProPacI introduced *Pme*I and *Pac*I restriction sites into the PGK2 promoter; and primers At1g79550ProPmeIFo and At1g79550-PromSpeIR introduced *Pme*I and *Spe*I restriction sites into the *PGK3* promoter). Subsequently, the *35S* promoters of constructs in pMDC83 were exchanged with the native promoters of *PGKs*, PCR amplified from pCAMBIA1303, and digested with the appropriate restriction enzymes. These vectors, called *ProPGK:PGKs*, were used for PGK expression and localization studies and for the complementation of *PGK1* and *PGK2* mutants. For *pgk3.2* complementation studies, the *Pro-35S:PGK3-GFP* construct in pMDC83 was used. Additionally, *pgk2.1* was transformed with a construct carrying a 3,718-bp genomic fragment that was PCR amplified from the bacterial artificial chromosome *F14G9* using primers At1g56190ForGENO and At1g56190RevGENO. This fragment, including 1,466 nucleotides upstream of the ATG, was cloned in the pCR8/GW/TOPO plasmid (Invitrogen) and subsequently subcloned in the plasmid pMDC99 (Curtis and Grossniklaus, 2003) using Gateway technology with Clonase II (Invitrogen).

The amiRNAs were produced to target *PGK1* and *PGK2* using the Web microRNA designer (http://wmd2.weigelworld.org/cgi-bin/mirnatools.pl). The amiRNAs were cloned according to the protocol by Rebecca Schwab in D. Weigel's laboratory (http://wmd2.weigelworld.org/themes/amiRNA/pics/Cloning_of_artificial_microRNAs.pdf) using primers listed in Supplemental Table S6, then placed in the pCR8/GW/TOPO plasmid (Invitrogen), and finally subcloned in the plasmid pMDC83 behind the *35S* promoter (Curtis and Grossniklaus, 2003). All PCR-derived constructs were verified by DNA sequencing.

Various Arabidopsis wild-type and mutant lines were transformed with the different constructs by the floral dipping method (Clough and Bent, 1998) with *Agrobacterium tumefaciens* carrying *pSOUP*. For the amiRNA and GUS lines, wild-type plants were used. Transformants were selected by antibiotic selection, while homozygous individuals in complementation studies were identified by PCR genotyping using gene-specific primers and left border primers of the T-DNA insertions listed in Supplemental Table S6. At least four independent single-insertion homozygous T3 lines were obtained for all different constructs. After characterization by RT-PCR, two different lines were selected for further analyses according to their expression levels. We used both syngenic wild-type lines as well as wild-type Columbia-0 as controls for our studies. For amiRNAs, we used the wild type used for transformation with the amiRNAs as controls.

### RT-PCR and RNA-seq Data

RT-PCR was performed as described previously (Cascales-Miñana et al., 2013). Each reaction was performed in triplicate with 1 $\mu$L of the first-strand cDNA in a total volume of 25 $\mu$L. Data are means of three biological samples. The specificity of the PCR amplification was confirmed with a heat dissociation curve (from 60°C to 95°C). The efficiency of the PCR was calculated, and different internal standards were selected (Czechowski et al., 2005) depending on the efficiency of the primers. Primers used are listed in Supplemental Table S6.

For the gene expression analysis by RNA-seq, 21-d-old wild-type plants grown vertically on 1/5 MS plates were used. Three independent biological replicates of wild-type AP and roots were used for the analysis. Total RNA was extracted using the NucleoSpin RNA II kit (Macherey-Nagel). Using as starting material 3 to 15 $\mu$g of RNA, an mRNA enrichment was performed with the MicroPoly(A) Purist kit (Ambion). To prepare the RNA-Seq library, the SOLID Total RNA-seq kit (Life Technologies) was used. After obtaining the library, an equimolar mixture of it was used to perform an emulsion PCR using the automatic system of EZ Beads (Life Technologies). Then, the bead enrichment was performed followed by its deposition in the sequencing wells. The sequencing step was done by SOLID 5500XL equipment of 75 nucleotides using the Exact Call Chemistry. To filtrate the readings depending on their adaptor, the Cutadapt version 1.8 program was used. FastqQC was employed to evaluate the quality of the reads. Afterward, Tophat2 was employed to perform the mapping against a reference. To visualize and obtain the raw counts, Seqmonk version 0.29 was used.

### GUS Activity Assays and GFP Microscopy

GUS activity assays were performed as described by Muñoz-Bertomeu et al. (2009). GFP fluorescence was observed with a confocal microscope (Leica TCS-SP). To confirm the nuclear localization of PGK3, root cells were stained with 10 $\mu$g $mL^{-1}$ Hoechst dye.

## Photosynthetic Activity Measurements

Simultaneous gas-exchange and chlorophyll fluorescence measurements were performed as described by Faus et al. (2015). Measurements were taken 2 h after the beginning of the light period to allow full photosynthesis activation.

## Metabolite Determination and PGK Activity Assay

The AP and roots of the wild type, single and double mutants, and silenced lines (two different lines per silenced gene), grown on 1/5 MS plates, were used to determine metabolite content in derivatized methanol extracts by gas chromatography-mass spectrometry using the protocol defined by Lisec et al. (2006). Metabolites were identified in comparison with database entries of authentic standards (Kopka et al., 2005). Chromatograms and mass spectra were evaluated using Chroma TOF 1.0 (LECO) and TagFinder 4.0 software (Luedemann et al., 2008). Material was sampled for metabolite analysis after 4 to 6 h in the light. 3-PGA was measured as described previously (Flores-Tornero et al., 2017). PGK activity was measured by an enzymatic assay following NADH oxidation associated with the coupled reaction of PGK and GAPDH. Frozen AP were ground in liquid nitrogen and resuspended in extraction buffer (50 mM HEPES-KOH, pH 7.4, 1 mM EDTA, 1 mM EGTA, 2 mM benzamidine, 2 mM ε-aminocaproic acid, 0.5 mM phenylmethylsulfonyl fluoride, 10% (v/v) glycerol, and 0.1% (v/v) Triton X-100). The supernatant was obtained after centrifugation at 15,000*g* for 20 min at 4°C. Reactions were carried out in a medium containing 100 mM HEPES-KOH, 1 mM EDTA, 2 mM $MgSO_4$, 0.3 mM NADH, 6.5 mM 3-PGA, 1 mM ATP, and 3.3 units of GAPDH. Starch was determined by the ENZYTEC starch kit (ATOM) at the end of the light period.

## Bioinformatics and Statistics

*PGK* and *TPT* genes were initially identified in The Arabidopsis Information Resource. The percentage identity between different PGKs was obtained by aligning pair sequences using bl2seq at the National Center for Biotechnology Information (http://blast.ncbi.nlm.nih.gov/Blast.cgi). Amino acid sequences were aligned using the ClustalOmega program (http://www.ebi.ac.uk/Tools/msa/clustalo/; McWilliam et al., 2013). Phylogenetic analyses were performed according to the neighbor-joining method (Saitou and Nei, 1987). Units represent the number of amino acid substitutions per site for one unit. The analysis was performed using the MEGA6 tool (Tamura et al., 2013).

Experimental values represent means and SE, and *n* represents the number of independent samples. Significant differences as compared with the wild type were analyzed by two-tailed Student's *t* tests algorithms using Microsoft Excel. Statistical differences between groups were analyzed with a one-way ANOVA and further posthoc Tukey's b test with the IBM SPSS Statistics software. The level of significance was fixed at 5% (0.05).

## Accession Numbers

The Arabidopsis Genome Initiative locus identifiers of Arabidopsis genes used in this article are as follows: At3g12780 (*PGK1*), At1g56190 (*PGK2*), At1g79550 (*PGK3*), and At5g46110 (*TPT*).

## Supplemental Data

The following supplemental materials are available.

**Supplemental Figure S1.** Amino acid alignment and cladogram of the Arabidopsis PGK proteins.

**Supplemental Figure S2.** Expression of GUS under the control of the *PGK1* promoter in seedlings and adult plants.

**Supplemental Figure S3.** Expression of GUS under the control of the *PGK2* promoter in seedlings and adult plants.

**Supplemental Figure S4.** *GUS* expression under the control of the *PGK3* promoter in seedlings and adult plants.

**Supplemental Figure S5.** Subcellular localization of PGK3 by stable expression of PGK-GFP fusion proteins under the control of the *35S* promoter.

**Supplemental Figure S6.** RT-PCR analysis of the AP of 20-d-old seedlings of *PGK2* and *PGK1* silenced lines grown on vertical plates.

**Supplemental Table S1.** Genomic localization of *PGK* family T-DNA mutant lines confirmed by sequencing.

**Supplemental Table S2.** Photosynthetic parameters in the wild type and two independent *amiPGK2* silenced lines.

**Supplemental Table S3.** Metabolite levels in the AP of 21-d-old *PGK* single and double mutants, silenced lines, and the wild type.

**Supplemental Table S4.** Metabolite levels in the roots of 21-d-old *PGK* single and double mutants, silenced lines, and the wild type.

**Supplemental Table S5.** Metabolite levels in the AP of 19-d-old *PGK3* and *TPT* single and double mutants and wild-type plants.

**Supplemental Table S6.** List of primers used in this work.

## ACKNOWLEDGMENTS

We thank Servei Central de Suport a la Investigación experimental (SCIE) and Unitat Central d'Investigació Medicina (UCIM) of the Universitat de València for technical assistance. We also thank Hellen Warburton for language review.

Received September 7, 2017; accepted September 22, 2017; published September 26, 2017.

## LITERATURE CITED

**Ai J, Huang H, Lv X, Tang Z, Chen M, Chen T, Duan W, Sun H, Li Q, Tan R, et al** (2011) FLNA and PGK1 are two potential markers for progression in hepatocellular carcinoma. Cell Physiol Biochem **27:** 207–216

**Alonso JM, Stepanova AN, Leisse TJ, Kim CJ, Chen H, Shinn P, Stevenson DK, Zimmerman J, Barajas P, Cheuk R, et al** (2003) Genome-wide insertional mutagenesis of *Arabidopsis thaliana*. Science **301:** 653–657

**Anderson LE, Advani VR** (1970) Chloroplast and cytoplasmic enzymes: three distinct isoenzymes associated with the reductive pentose phosphate cycle. Plant Physiol **45:** 583–585

**Anderson LE, Bryant JA, Carol AA** (2004) Both chloroplastic and cytosolic phosphoglycerate kinase isozymes are present in the pea leaf nucleus. Protoplasma **223:** 103–110

**Anoman AD, Muñoz-Bertomeu J, Rosa-Téllez S, Flores-Tornero M, Serrano R, Bueso E, Fernie AR, Segura J, Ros R** (2015) Plastidial glycolytic glyceraldehyde-3-phosphate dehydrogenase is an important determinant in the carbon and nitrogen metabolism of heterotrophic cells in Arabidopsis. Plant Physiol **169:** 1619–1637

**Archibald JM, Keeling PJ** (2003) Comparative genomics. Plant genomes: cyanobacterial genes revealed. Heredity (Edinb) **90:** 2–3

**Bläsing OE, Gibon Y, Günther M, Höhne M, Morcuende R, Osuna D, Thimm O, Usadel B, Scheible WR, Stitt M** (2005) Sugars and circadian regulation make major contributions to the global regulation of diurnal gene expression in *Arabidopsis*. Plant Cell **17:** 3257–3281

**Boer PH, Adra CN, Lau YF, McBurney MW** (1987) The testis-specific phosphoglycerate kinase gene *pgk-2* is a recruited retroposon. Mol Cell Biol **7:** 3107–3112

**Brice DC, Bryant JA, Dambrauskas G, Drury SC, Littlechild JA** (2004) Cloning and expression of cytosolic phosphoglycerate kinase from pea (*Pisum sativum* L.). J Exp Bot **55:** 955–956

**Brinkmann H, Martin W** (1996) Higher-plant chloroplast and cytosolic 3-phosphoglycerate kinases: a case of endosymbiotic gene replacement. Plant Mol Biol **30:** 65–75

**Cascales-Miñana B, Muñoz-Bertomeu J, Flores-Tornero M, Anoman AD, Pertusa J, Alaiz M, Osorio S, Fernie AR, Segura J, Ros R** (2013) The phosphorylated pathway of serine biosynthesis is essential both for male gametophyte and embryo development and for root growth in *Arabidopsis*. Plant Cell **25:** 2084–2101

**Chen M, Thelen JJ** (2010) The plastid isoform of triose phosphate isomerase is required for the postgerminative transition from heterotrophic to autotrophic growth in *Arabidopsis*. Plant Cell **22:** 77–90

**Cheng SF, Huang YP, Chen LH, Hsu YH, Tsai CH** (2013) Chloroplast phosphoglycerate kinase is involved in the targeting of *Bamboo mosaic virus* to chloroplasts in *Nicotiana benthamiana* plants. Plant Physiol **163:** 1598–1608

**Chiarelli LR, Morera SM, Bianchi P, Fermo E, Zanella A, Galizzi A, Valentini G** (2012) Molecular insights on pathogenic effects of mutations causing phosphoglycerate kinase deficiency. PLoS ONE **7:** e32065

**Clough SJ, Bent AF** (1998) Floral dip: a simplified method for *Agrobacterium*-mediated transformation of *Arabidopsis thaliana*. Plant J **16:** 735–743

**Curtis MD, Grossniklaus U** (2003) A Gateway cloning vector set for high-throughput functional analysis of genes in planta. Plant Physiol **133:** 462–469

**Czechowski T, Stitt M, Altmann T, Udvardi MK, Scheible WR** (2005) Genome-wide identification and testing of superior reference genes for transcript normalization in Arabidopsis. Plant Physiol **139:** 5–17

**Danshina PV, Geyer CB, Dai Q, Goulding EH, Willis WD, Kitto GB, McCarrey JR, Eddy EM, O'Brien DA** (2010) Phosphoglycerate kinase 2 (PGK2) is essential for sperm function and male fertility in mice. Biol Reprod **82:** 136–145

**Emanuelsson O, Nielsen H, von Heijne G** (1999) ChloroP, a neural network-based method for predicting chloroplast transit peptides and their cleavage sites. Protein Sci **8:** 978–984

**Faus I, Zabalza A, Santiago J, Nebauer SG, Royuela M, Serrano R, Gadea J** (2015) Protein kinase GCN2 mediates responses to glyphosate in *Arabidopsis*. BMC Plant Biol **15:** 14

**Fermani S, Sparla F, Falini G, Martelli PL, Casadio R, Pupillo P, Ripamonti A, Trost P** (2007) Molecular mechanism of thioredoxin regulation in photosynthetic A2B2-glyceraldehyde-3-phosphate dehydrogenase. Proc Natl Acad Sci USA **104:** 11109–11114

**Fischer K, Weber A** (2002) Transport of carbon in non-green plastids. Trends Plant Sci **7:** 345–351

**Flores-Tornero M, Anoman AD, Rosa-Téllez S, Toujani W, Weber AP, Eisenhut M, Kurz S, Alseekh S, Fernie AR, Muñoz-Bertomeu J, et al** (2017) Overexpression of the triose phosphate translocator (TPT) complements the abnormal metabolism and development of plastidial glycolytic glyceraldehyde-3-phosphate dehydrogenase mutants. Plant J **89:** 1146–1158

**Guo L, Devaiah SP, Narasimhan R, Pan X, Zhang Y, Zhang W, Wang X** (2012) Cytosolic glyceraldehyde-3-phosphate dehydrogenases interact with phospholipase Dδ to transduce hydrogen peroxide signals in the *Arabidopsis* response to stress. Plant Cell **24:** 2200–2212

**Guo L, Ma F, Wei F, Fanella B, Allen DK, Wang X** (2014) Cytosolic phosphorylating glyceraldehyde-3-phosphate dehydrogenases affect *Arabidopsis* cellular metabolism and promote seed oil accumulation. Plant Cell **26:** 3023–3035

**Hajirezaei MR, Biemelt S, Peisker M, Lytovchenko A, Fernie AR, Sonnewald U** (2006) The influence of cytosolic phosphorylating glyceraldehyde 3-phosphate dehydrogenase (GAPC) on potato tuber metabolism. J Exp Bot **57:** 2363–2377

**Han S, Wang Y, Zheng X, Jia Q, Zhao J, Bai F, Hong Y, Liu Y** (2015) Cytoplastic glyceraldehyde-3-phosphate dehydrogenases interact with ATG3 to negatively regulate autophagy and immunity in *Nicotiana benthamiana*. Plant Cell **27:** 1316–1331

**Holtgrefe S, Gohlke J, Starmann J, Druce S, Klocke S, Altmann B, Wojtera J, Lindermayr C, Scheibe R** (2008) Regulation of plant cytosolic glyceraldehyde 3-phosphate dehydrogenase isoforms by thiol modifications. Physiol Plant **133:** 211–228

**Hwang TL, Liang Y, Chien KY, Yu JS** (2006) Overexpression and elevated serum levels of phosphoglycerate kinase 1 in pancreatic ductal adenocarcinoma. Proteomics **6:** 2259–2272

**Joshi R, Karan R, Singla-Pareek SL, Pareek A** (2016) Ectopic expression of Pokkali phosphoglycerate kinase-2 (OsPGK2-P) improves yield in tobacco plants under salinity stress. Plant Cell Rep **35:** 27–41

**Kopka J, Schauer N, Krueger S, Birkemeyer C, Usadel B, Bergmüller E, Dörmann P, Weckwerth W, Gibon Y, Stitt M, et al** (2005) GMD@CSB. DB: the Golm Metabolome Database. Bioinformatics **21:** 1635–1638

**Köpke-Secundo E, Molnar I, Schnarrenberger C** (1990) Isolation and characterization of the cytosolic and chloroplastic 3-phosphoglycerate kinase from spinach leaves. Plant Physiol **93:** 40–47

**Krietsch WK, Bücher T** (1970) 3-Phosphoglycerate kinase from rabbit skeletal muscle and yeast. Eur J Biochem **17:** 568–580

**Lay AJ, Jiang XM, Kisker O, Flynn E, Underwood A, Condron R, Hogg PJ** (2000) Phosphoglycerate kinase acts in tumour angiogenesis as a disulphide reductase. Nature **408:** 869–873

**Lin JW, Ding MP, Hsu YH, Tsai CH** (2007) Chloroplast phosphoglycerate kinase, a gluconeogenetic enzyme, is required for efficient accumulation of *Bamboo mosaic virus*. Nucleic Acids Res **35:** 424–432

**Lisec J, Schauer N, Kopka J, Willmitzer L, Fernie AR** (2006) Gas chromatography mass spectrometry-based metabolite profiling in plants. Nat Protoc **1:** 387–396

**Liu D, Li W, Cheng J, Hou L** (2015) *AtPGK2,* a member of PGKs gene family in Arabidopsis, has a positive role in salt stress tolerance. Plant Cell Tissue Organ Cult **120:** 251–262

**Löbler M** (1998) Two phosphoglycerate kinase cDNAs from *Arabidopsis thaliana*. DNA Seq **8:** 247–252

**Longstaff M, Raines CA, McMorrow EM, Bradbeer JW, Dyer TA** (1989) Wheat phosphoglycerate kinase: evidence for recombination between the genes for the chloroplastic and cytosolic enzymes. Nucleic Acids Res **17:** 6569–6580

**Luedemann A, Strassburg K, Erban A, Kopka J** (2008) TagFinder for the quantitative analysis of gas chromatography-mass spectrometry (GC-MS)-based metabolite profiling experiments. Bioinformatics **24:** 732–737

**McCarrey JR, Thomas K** (1987) Human testis-specific PGK gene lacks introns and possesses characteristics of a processed gene. Nature **326:** 501–505

**McCormick AJ, Kruger NJ** (2015) Lack of fructose 2,6-bisphosphate compromises photosynthesis and growth in Arabidopsis in fluctuating environments. Plant J **81:** 670–683

**McMorrow EM, Bradbeer JW** (1990) Separation, purification, and comparative properties of chloroplast and cytoplasmic phosphoglycerate kinase from barley leaves. Plant Physiol **93:** 374–383

**McWilliam H, Li W, Uludag M, Squizzato S, Park YM, Buso N, Cowley AP, Lopez R** (2013) Analysis Tool Web Services from the EMBL-EBI. Nucleic Acids Res **41:** W597–W600

**Morisse S, Michelet L, Bedhomme M, Marchand CH, Calvaresi M, Trost P, Fermani S, Zaffagnini M, Lemaire SD** (2014) Thioredoxin-dependent redox regulation of chloroplastic phosphoglycerate kinase from *Chlamydomonas reinhardtii*. J Biol Chem **289:** 30012–30024

**Muñoz-Bertomeu J, Cascales-Miñana B, Irles-Segura A, Mateu I, Nunes-Nesi A, Fernie AR, Segura J, Ros R** (2010) The plastidial glyceraldehyde-3-phosphate dehydrogenase is critical for viable pollen development in Arabidopsis. Plant Physiol **152:** 1830–1841

**Muñoz-Bertomeu J, Cascales-Miñana B, Mulet JM, Baroja-Fernández E, Pozueta-Romero J, Kuhn JM, Segura J, Ros R** (2009) Plastidial glyceraldehyde-3-phosphate dehydrogenase deficiency leads to altered root development and affects the sugar and amino acid balance in Arabidopsis. Plant Physiol **151:** 541–558

**Myouga F, Akiyama K, Motohashi R, Kuromori T, Ito T, Iizumi H, Ryusui R, Sakurai T, Shinozaki K** (2010) The Chloroplast Function Database: a large-scale collection of Arabidopsis *Ds/Spm-* or T-DNA-tagged homozygous lines for nuclear-encoded chloroplast proteins, and their systematic phenotype analysis. Plant J **61:** 529–542

**Ouibrahim L, Mazier M, Estevan J, Pagny G, Decroocq V, Desbiez C, Moretti A, Gallois JL, Caranta C** (2014) Cloning of the Arabidopsis *rwm1* gene for resistance to *Watermelon mosaic virus* points to a new function for natural virus resistance genes. Plant J **79:** 705–716

**Paul MJ, Pellny TK** (2003) Carbon metabolite feedback regulation of leaf photosynthesis and development. J Exp Bot **54:** 539–547

**Petersen J, Brinkmann H, Cerff R** (2003) Origin, evolution, and metabolic role of a novel glycolytic GAPDH enzyme recruited by land plant plastids. J Mol Evol **57:** 16–26

**Plaxton WC** (1996) The organization and regulation of plant glycolysis. Annu Rev Plant Physiol Plant Mol Biol **47:** 185–214

**Popanda O, Fox G, Thielmann HW** (1998) Modulation of DNA polymerases α, δ and ε by lactate dehydrogenase and 3-phosphoglycerate kinase. Biochim Biophys Acta **1397:** 102–117

**Prabhakar V, Löttgert T, Geimer S, Dörmann P, Krüger S, Vijayakumar V, Schreiber L, Göbel C, Feussner K, Feussner I, et al** (2010) Phosphoenolpyruvate provision to plastids is essential for gametophyte and sporophyte development in *Arabidopsis thaliana*. Plant Cell **22:** 2594–2617

**Rius SP, Casati P, Iglesias AA, Gomez-Casati DF** (2006) Characterization of an *Arabidopsis thaliana* mutant lacking a cytosolic non-phosphorylating glyceraldehyde-3-phosphate dehydrogenase. Plant Mol Biol **61:** 945–957

**Saitou N, Nei M** (1987) The neighbor-joining method: a new method for reconstructing phylogenetic trees. Mol Biol Evol **4:** 406–425

**Sambrook J, Russell DW** (2001) Molecular Cloning: A Laboratory Manual, Ed 3. Cold Spring Harbor Laboratory Press, Cold Spring Harbor, NY

**Scholl RL, May ST, Ware DH** (2000) Seed and molecular resources for Arabidopsis. Plant Physiol **124:** 1477–1480

**Shih MC, Lazar G, Goodman HM** (1986) Evidence in favor of the symbiotic origin of chloroplasts: primary structure and evolution of tobacco glyceraldehyde-3-phosphate dehydrogenases. Cell **47:** 73–80

**Smith AM, Stitt M** (2007) Coordination of carbon supply and plant growth. Plant Cell Environ **30:** 1126–1149

**Sparla F, Zaffagnini M, Wedel N, Scheibe R, Pupillo P, Trost P** (2005) Regulation of photosynthetic GAPDH dissected by mutants. Plant Physiol **138:** 2210–2219

**Staehr P, Löttgert T, Christmann A, Krueger S, Rosar C, Rolčík J, Novák O, Strnad M, Bell K, Weber AP, et al** (2014) Reticulate leaves and stunted roots are independent phenotypes pointing at opposite roles of the phosphoenolpyruvate/phosphate translocator defective in cue1 in the plastids of both organs. Front Plant Sci **5:** 126

**Stitt M, Lunn J, Usadel B** (2010) Arabidopsis and primary photosynthetic metabolism: more than the icing on the cake. Plant J **61:** 1067–1091

**Tamura K, Stecher G, Peterson D, Filipski A, Kumar S** (2013) MEGA6: Molecular Evolutionary Genetics Analysis version 6.0. Mol Biol Evol **30:** 2725–2729

**Troncoso-Ponce MA, Garcés R, Martínez-Force E** (2010) Glycolytic enzymatic activities in developing seeds involved in the differences between standard and low oil content sunflowers (*Helianthus annuus* L.). Plant Physiol Biochem **48:** 961–965

**Troncoso-Ponce MA, Kruger NJ, Ratcliffe G, Garcés R, Martínez-Force E** (2009) Characterization of glycolytic initial metabolites and enzyme activities in developing sunflower (*Helianthus annuus* L.) seeds. Phytochemistry **70:** 1117–1122

**Troncoso-Ponce MA, Rivoal J, Venegas-Calerón M, Dorion S, Sánchez R, Cejudo FJ, Garcés R, Martínez-Force E** (2012) Molecular cloning and biochemical characterization of three phosphoglycerate kinase isoforms from developing sunflower (*Helianthus annuus* L.) seeds. Phytochemistry **79:** 27–38

**Wakao S, Chin BL, Ledford HK, Dent RM, Casero D, Pellegrini M, Merchant SS, Niyogi KK** (2014) Phosphoprotein SAK1 is a regulator of acclimation to singlet oxygen in *Chlamydomonas reinhardtii*. eLife **3:** e02286

**Willard HF, Goss SJ, Holmes MT, Munroe DL** (1985) Regional localization of the phosphoglycerate kinase gene and pseudogene on the human X chromosome and assignment of a related DNA sequence to chromosome 19. Hum Genet **71:** 138–143

**Zhao Z, Assmann SM** (2011) The glycolytic enzyme, phosphoglycerate mutase, has critical roles in stomatal movement, vegetative growth, and pollen production in *Arabidopsis thaliana*. J Exp Bot **62:** 5179–5189

**Zieker D, Königsrainer I, Traub F, Nieselt K, Knapp B, Schillinger C, Stirnkorb C, Fend F, Northoff H, Kupka S, et al** (2008) PGK1 a potential marker for peritoneal dissemination in gastric cancer. Cell Physiol Biochem **21:** 429–436

**Zieker D, Königsrainer I, Weinreich J, Beckert S, Glatzle J, Nieselt K, Bühler S, Löffler M, Gaedcke J, Northoff H, et al** (2010) Phosphoglycerate kinase 1 promoting tumor progression and metastasis in gastric cancer: detected in a tumor mouse model using positron emission tomography/magnetic resonance imaging. Cell Physiol Biochem **26:** 147–154